Accepted Manuscript

Efficient ceria-zirconium oxide catalyst for carbon dioxide conversions: Characterization, catalytic activity and thermodynamic study

Praveen Kumar, Patrick With, Vimal Chandra Srivastava, Roger Gläser, Indra Mani Mishra

PII: S0925-8388(16)33430-2

DOI: 10.1016/j.jallcom.2016.10.293

Reference: JALCOM 39462

To appear in: *Journal of Alloys and Compounds*

Received Date: 1 May 2016

Revised Date: 13 September 2016

Accepted Date: 29 October 2016

Please cite this article as: P. Kumar, P. With, V.C. Srivastava, R. Gläser, I.M. Mishra, Efficient ceria-zirconium oxide catalyst for carbon dioxide conversions: Characterization, catalytic activity and thermodynamic study, *Journal of Alloys and Compounds* (2016), doi: 10.1016/j.jallcom.2016.10.293.

Efficient ceria-zirconium oxide catalyst for carbon dioxide conversions: characterization, catalytic activity and thermodynamic study

Praveen Kumar [a,c*], Patrick With[b], Vimal Chandra Srivastava[a], Roger Gläser [c], Indra Mani Mishra[a,d]

[a]Department of Chemical Engineering, Indian Institute of Technology Roorkee, Roorkee 247667, Uttarakhand, India
[b]Leibniz-Institutes für Oberflächenmodifizierung e. V. (IOM), Permoserstr. 15, D-04318 Leipzig, Germany
[c]Institute of Chemical Technology, Universität Leipzig, Linnéstraße 3, 04103 Leipzig, Germany
[d]Department of Chemical Engineering, Indian Institute of Technology (Indian School of Mines), Dhanbad - 826004, Jharkhand, India

***Corresponding Author:** Phone: +91–1332–285889; fax: +91–1332–276535. **E–mail addresses**: praveen.zon@gmail.com, praveen.singh@daad-alumni.de (P. Kumar)

Abstract

In this study, ceria-zirconia based catalysts (CeO_2, ZrO_2 and $Ce_{0.5}Zr_{0.5}O_2$) catalysts were synthesized by hydrothermal method and characterized by N_2-sorption, X-ray diffraction (XRD), scanning electron microscopy (SEM) and transmission electron microscopy (TEM). Acidity and basicity of synthesized catalysts have been investigated by NH_3- and CO_2- temperature-programmed desorption (TPD). Brunauer-Emmett-Teller (BET) surface area of CeO_2, $Ce_{0.5}Zr_{0.5}O_2$ and ZrO_2 were found to be 88, 117 and 70 $m^2\ g^{-1}$ and average crystalline sizes was 9.48, 7.09 and 9.45 nm, respectively. These catalysts were further used for direct conversion of CO_2 with methanol for the synthesis of dimethyl carbonate (DMC). DMC yield was found to be highly dependent upon the both basicity and acidity of catalysts. $Ce_{0.5}Zr_{0.5}O_2$ catalysts showed better activity as compared to CeO_2 and ZrO_2 catalyst. Effect of reaction conditions (such as catalysts dose, reaction temperature and reaction time) and catalyst reusability was studied with $Ce_{0.5}Zr_{0.5}O_2$ catalyst. The optimum operating condition for direct conversion of CO_2 into DMC at constant pressure 150 bar, reaction time=24 h, catalyst dose=1.25 g and temperature=120 °C. Moreover, chemical

equilibrium modeling has been performed using Peng–Robinson–Stryjek–Vera equation of state (PRSV-EoS) along with the van der Waals one-fluid (1PVDW) mixing rule to calculate heat of reaction and Gibbs free energy change.

Keywords: DMC; direct conversion of CO_2; $Ce_{0.5}Zr_{0.5}O_2$ catalyst; NH_3- & CO_2-TPD.

1. Introduction

Dimethyl carbonate (DMC) is a promising chemical in alkyl carbonate series, due to its non-toxic and biodegradable nature. It is high versatile in terms of its usage and is widely used for green chemical synthesis [1-3]. It can be used as a solvent for synthesis of various useful chemicals such as copolymers, phenol carbonate [4], polycyclic aromatic [5], etc. It is also used in electrolytic solution in lithium battery due to high dielectric constant [5]. DMC is used as a replacement of non-biodegradable and toxic methyl tert-butyl ether (MTBE) additive in the gasoline based fuels [6]. DMC has high oxygen content (53.3%) as compared to other commercial fuel additives such as methyl tert-butyl ether (MTBE) (17.6%), ethanol (34.89%) and methanol (50%) and is consequently used as octane booster in gasoline based fuels [1-3]. Traditionally, DMC was synthesized by various methods such as phosgenation process, oxycarbonylation and methyl nitrite carbonylation process [1-3,7-8]. Other methods used for DMC synthesis such as the direct synthesis from CO_2, transesterification of propylene carbonate and urea methanolysis process are also used for synthesis of DMC [9-13].

In the last few years, CO_2 is considered as an abundant, cheap, non-toxic and inexpensive renewable resource which can be utilized for the synthesis of a variety of chemicals. However, the transformation of CO_2 to other valuable products requires high energy [14-16]. Consequently various catalysts are being used to lower this energy requirement and enhance the productivity using different routes [14-17]. Methods are also

being developed for transformation of CO_2 into DMC in the presence of a catalyst. However, this route of CO_2 utilization requires a lot of research attention due to very low DMC yield because of thermodynamic restrictions (ΔH=16.74 kJ/mol) [18]. Various homogeneous catalysts such as thallium (I) hydroxide, tin (IV) tetralkoxides, dialkytin dialkoxides, bases, C,N-chelated organotin (IV) trifluoro methane sulfonates and titanium (IV) tetralkoxides have been used for the synthesis of DMC from CO_2 [19-25]. Deactivation of catalyst, difficult separation process, and recovery of catalyst, etc. are some of the drawbacks of homogeneous systems. Subsequently, various heterogeneous catalyst have been investigated for DMC synthesis such as CeO_2 [26], ZrO_2 [26], $Ce_{0.5}Zr_{0.5}O_2$ [27-28], Gd-$Ce_{0.4}Zr_{0.6}O_2$ [28], Cu-CeO_2 [29], Sn-SBA-15 [30], and C,N-chelated organotin (IV) trifluoro methane sulfonates [19] have been reported for DMC synthesis. Few investigators have previously used CeO_2, ZrO_2 and combined CeO_2-ZrO_2 catalysts for DMC synthesis from CO_2 [26-28]. Zhang et al. [27] synthesized and characterized $Ce_{0.5}Zr_{0.5}O_2$ catalyst and used it for DMC synthesis from CO_2. However, Lee et al. [28] synthesized $Ce_{0.4}Zr_{0.6}O_2$ catalysts by sol-gel method and metal oxides (Ga_2O_3, La_2O_3, Ni_2O_3, Fe_2O_3, Y_2O_3, Co_3O_4, and Al_2O_3) were further supported on $Ce_{0.6}Zr_{0.4}O_2$ by an incipient wetness impregnation method and used as catalysts for DMC synthesis. Authors correlated the amount of DMC formed mmol/g-catalyst with basicity and acidity of the catalysts. Chen et al. [26] used CeO_2 and ZrO_2 catalysts for direct conversion of CO_2 with methanol into DMC and studied their reaction mechanism. Synthesis of DMC from CO_2 is one of the primary utilization routes and interest CeO_2-ZrO_2 solid solutions have been demonstrated in the literature to have good catalytic properties.

It is known that for commercialization of this route is essential to optimize the operating parameters such as catalysts dose, reaction temperature and reaction time and study the reusability of the catalysts. All these factors have been studied in the present study and

discussed with respect to catalyst characterization. Moreover, present study reports chemical equilibrium modeling which is essential for reactor design.

In the present work, synthesis of DMC from direct conversion of CO_2 with methanol was studied using ceria, zirconia and ceria-zirconia catalysts prepared by hydrothermal method. Synthesized catalysts were characterized by liquid N_2-sorption, X-ray diffraction (XRD), atomic force microscopy (AFM), scanning electron microscopy (SEM), and transmission electron microscopy (TEM). Acidity and basicity of synthesized catalysts have been investigated by NH_3- and CO_2-temperature-programmed desorption (TPD). Effect of the reaction condition such as catalysts dose, reaction temperature, reaction time and reusability of the catalyst was studied with chemical equilibrium modeling using best performing catalyst.

2. Experimental

2.1 Materials

Cerium (III) nitrate hexahydrate ($Ce(NO_3)_3.6H_2O$) 99.0%, and zirconium (IV) oxychloride octahydrate ($ZrOCl_2.8H_2O$) 99.0% were purchased from Sigma Aldrich Chemicals, GmbH. Ammonia solution (25 wt% in H_2O) was purchased from Merck GmbH. Dimethyl carbonate (DMC) 99.9% and methanol (99.0%) were purchased from Sigma Aldrich Chemicals, GmbH. All chemicals used were of analytical grade (AR) without further purification. Deionized water was obtained from Milli-Q water filtration station (Millipore).

2.2. Catalyst Preparation

CeO_2, $Ce_{0.5}Zr_{0.5}O_2$ and ZrO_2 catalyst were synthesized from $Ce(NO_3)_3.6H_2O$ and $ZrOCl_2.8H_2O$ salts using hydrothermal method. $Ce(NO_3)_3.6H_2O$ (0, 6, 12 mmol) and $ZrOCl_2.8H_2O$ (12, 6, 0 mmol) were dissolved separately in 50 cm^3 ethanol and further mixed together in desired molar ratio under continuous stirring at room temperature. Liquid

ammonia solution was added drop-wise in the mixed metal solution over a period until the pH reached ~9.5. Further, the formed solution was aged for 4 h. Yellow mixed solution obtained after the reaction were introduced in 100 mL teflon-lined autoclave and kept in 120 °C for 24 h, then cooled to room temperature naturally. Yellow colour slurry obtained was washed several times with double distilled water with acetone until pH became neutral. Resulting precipitate was dried at 110 °C for 24 h in air. Finally, the fresh samples were calcined at 500 °C for 4 h in air atmosphere to obtain the CeO_2, $Ce_{0.5}Zr_{0.5}O_2$ and ZrO_2 catalysts. The synthesized catalysts were denoted as CeO_2, $Ce_{0.5}Zr_{0.5}O_2$ and ZrO_2 catalyst having pure CeO_2, mixed CeO_2-ZrO_2 and pure ZrO_2, respectively.

2.3 Catalyst characterization

Synthesized catalysts were characterized by X-ray diffraction pattern (XRD), N_2-sorption, temperature programmed desorption (TPD) of CO_2 and NH_3, scanning electron microscope-energy disperse X-ray (SEM-EDX).

The crystallographic structure of samples was examined using Siemens D5000 diffractometer with Cu-Kα radiation (λ=0.15406 nm) over 2θ range of 5° - 80° with a step size of 0.02° at 40 kV. Crystalline phases were analyzed using PANalytical X'pertHigh Score software with the database in the JCPDS (Joint Committee of Powder Diffraction Standards). Scherrer equation used for the calculating the average crystalline sizes.

$$L = \frac{K\lambda}{(\beta_{sample} - \beta_{standard})cos\theta} \quad (1)$$

where, L is the average particle size, K is the Scherrer's constant (0.94), λ is the X-ray radiation of wavelength of which is equal to 0.154051 nm, β is the full width of the reflection at half maximum (FWHM) and θ is the Bragg angle. High grade silicon powder was used as an internal standard for the instrument broadening correction **[31]**.

Morphology of the sample and its elemental compositions were analyzed using QUANTA, Model 200 FEG, Netherlands equipped with EDX on gold coated samples. The

TEM characterization was study using TECNAI G^2 20S-TWIN, FEI Netherlands with LaB_6 as cathode (resolution: point 0.24 nm and line 0.14 nm) at 200 kV. The samples were dispersed with ethanol and sonicated for 60 min and then drop deposited on the copper micro-grid and dried at room temperature for 2 h.

Textural properties of the samples were measured at -195 °C using Micromeritics ASAP 2020 apparatus by N_2 adsorption/desorption. Sample was degassed for 8 h at 200 °C under vacuum to remove any absorbed impurities before performing the experiments. Brunauer-Emmett-Teller (BET) method used for determined the surface area of the sample in the range of relative pressure 0.05 to 0.35 [32] and Barrett-Joyner-Halenda (BJH) method used for calculating the pore area and pore volume [33] using the desorption section of nitrogen isotherms.

Basicity of the samples were determined using CO_2-TPD experiment using Micromeritics Chemisorb 2720 instrument coupled with a thermal conductivity detector (TCD). The sample (100 mg) pretreated at 200 °C under helium flow (20 cm^3 min^{-1}) for 6 h and then exposed to CO_2 stream with a flow rate 20 ml min^{-1} for 30 min at room temperature and physisorbed CO_2 was removed by helium purging for 1 h at room temperature. Then, the temperature was increased with heating rate of 10 °C min^{-1} under helium flow (20 cm^3 min^{-1}) from 50 - 700 °C and the desorbed CO_2 was monitored by TCD, which was calibrated by injections of pure CO_2 pulses. Similarly, same process was applied for NH_3-TPD to determine the acidity and acidic strength of the sample.

Morphology and grain size distribution of the catalysts was also studied using atomic force microscopy (AFM) by NT-MDT M/s Molecular Tools and Devices for Nanotechnology and NOVA software used for image analysis. Sample were prepared in ethanol, the small amount of sample was dispersed in ethanol solution and solution was sonicated for 180 min.

Afterwards, small amount of solution was placed on a glass plate and dried at room temperature for 12 h. Then this glass plate was used for AFM analysis.

2.4. Catalytic activity

Catalytic activity of the synthesized catalysts was checked for the synthesis of DMC from direct conversion of CO_2 with methanol in a stainless-steel autoclave reactor. Reactor was initially filled with required amounts of methanol and the catalysts. The reactor was heated at reaction temperature (100-180 °C) and pressurizing with CO_2 with the reaction pressure (150 bar). After (6-48 h), the reactor was kept in an ice bath so as to cool down the product mixture to (<−20 °C) and thereafter catalyst was separated from the mixture by centrifugation. All the reactions were studied in the presence of activated molecular sieve 3A as a dehydrating agent and at constant stirrer speed of 600 min^{-1}. Catalyst was washed with methanol and dried at 150 °C for 12 h and further activated at 500 $^{\circ}$C for 4 h after each cycle. Similalrly, molecular sieves was activated at 240 °C for 4 h after each cycle.

The product was analyzed by gas chromatograph (GC) HP 5890 equipped with a capillary column HP-5 (5%-phenyl)-methyl polysiloxane with a length of 30 m, an inner diameter of 0.25 mm and a film thickness of 1.8 microns with a flame ionization detector (FID). Injector and detector temperature were 220 and 250 °C, respectively. Helium gas was used as a carrier gas with flow rate 30 ml/min. Initial column temperature was 40 °C with holding time 5 min. After that, temperature was ramped to 100 °C where it was held for 5 min thereafter temperature was ramped to 220 °C at the rate of 10 °C/min where it was held for 5 min.

3. Results and Discussion

3.1 Catalyst Characterization

XRD profiles of CeO_2, $Ce_{0.5}Zr_{0.5}O_2$ and ZrO_2 catalysts are presented in Fig. 1. XRD pattern of CeO_2 catalysts shows the reflections of cubic phase (JPDS File No. 01-074-1145) with space group Fm3m (225), ZrO_2 catalysts shows the reflections of tetragonal phase (JPDS File No. 01-080-2155) with space group P42/nmc (137) and $Ce_{0.5}Zr_{0.5}O_2$ reflections show tetragonal phase (JPDS File No. 00-038-1436) with space group P42/nmc (137). Only pure phases were found in CeO_2 and ZrO_2. $Ce_{0.5}Zr_{0.5}O_2$ catalysts showed the presence of $Ce_{0.5}Zr_{0.5}O_2$ (JPDS File No. 00-038-1436). XRD reflections get shifted in the mixed solid solution due to difference in the ionic radii of Ce^{4+} (0.097 nm) and Zr^{4+} (0.084 nm). Average crystallite sizes of CeO_2, ZrO_2 and $Ce_{0.5}Zr_{0.5}O_2$ were determined from the most intensive reflections at 2θ=28.5°, 30.2° and 29.2°, respectively. Average crystalline sizes of the CeO_2, $Ce_{0.5}Zr_{0.5}O_2$ and ZrO_2 catalysts were 9.48, 7.09 and 9.45 nm, respectively. Additionally, a TEM image of the $Ce_{0.5}Zr_{0.5}O_2$ catalysts shows spherical particles in the range of 7-12 nm. SAED indexing pattern confirms the presence of the crystalline phases identified using XRD in $Ce_{0.5}Zr_{0.5}O_2$. Several investigators have previously reported similar XRD results for CeO_2, ZrO_2 and $Ce_{0.5}Zr_{0.5}O_2$. Chen et al. [26] reported cubic phase of CeO_2 and tetragonal phase of ZrO_2 whereas Zhang et al. [27] reported that the $Ce_{0.5}Zr_{0.5}O_2$ samples calcined at 773 K were quite similar (cubic phase with crystal sizes of ≈2.6 nm), while the samples calcined at 1273 contained both cubic and tetragonal phases, irrespective of the complexing agents used. Fuentes and Baker [31] reported either a cubic (Fm3m) or a tetragonal (P42/nmc) phase depending on Ce content in $Ce_xZr_{1-x}O_2$ (x = 0.1, 0.25, 0.5, 0.75, and 0.9) prepared using a citrate complexation technique. Similarly, Si et al. [34] and Roh et al. [35] reported average crystalline size of 5-6 with cubic and tetragonal mixed phase of $Ce_{0.5}Zr_{0.5}O_2$. Atribak et al., [36, 37] have been reported average crystalline sizes 11 nm of mixed phase of $Ce_{0.76}Zr_{0.24}O_2$ catalyst. In the present study, the Ce/Zr molar ratios in the $Ce_{0.5}Zr_{0.5}O_2$ mixed oxides catalyst were determined by ICP-OES analysis and EDX analysis. Structural chemical compositions

of the catalysts are shown in Table S1 (supporting information). Formation of chemical compositions of synthesized catalysts was relatively close to the initial mixed metal composition.

SEM was performed on CeO_2, $Ce_{0.5}Zr_{0.5}O_2$ and ZrO_2 synthesized catalysts and obtained micrographs are shown in Fig. 4. All the catalysts show spherical morphology. Average particle size of the all the catalysts as investigated from FE-SEM is found to be in the range of 5-10 nm. ZrO_2 is of smaller size as compared to $Ce_{0.5}Zr_{0.5}O_2$ catalyst (Fig. 4). $Ce_{0.5}Zr_{0.5}O_2$ mapping shown in Fig. S1 shows homogeneous dispersion of metals in all the catalysts. The surface morphology was further investigated by AFM. AFM (1D and 3D) images along with grain size distribution of the $Ce_{0.5}Zr_{0.5}O_2$ catalyst is shown in Fig. S2. Average grain size was found to be ~4.5 nm. Surface roughness values obtained from AFM analysis was 0.945 nm.

The pore surface area of catalysts was calculated according to the BET methods and pore size and pore volume was calculated by BJH method. N_2 adsorption-desorption isotherm and pore size distribution are shown in Fig. 2. Textural data of the catalysts are given in Table 1. BET surface area of CeO_2, $Ce_{0.5}Zr_{0.5}O_2$ and ZrO_2 were found to be 88, 117 and 70 $m^2\ g^{-1}$, respectively, BJH desorption pore volume and average pore diameter was in the range of 0.12 - 0.237 $cm^3\ g^{-1}$ and 5 - 8.41 nm, respectively. $Ce_{0.5}Zr_{0.5}O_2$ catalyst was found to posses the highest surface area, specific pore volume and average pore diameter among all the synthesized catalysts. Different authors have reported varied BET surface area (5-134 m^2/g) of $Ce_{0.5}Zr_{0.5}O_2$ catalysts [27-28, 31, 34-38]. All catalysts showed type VI isotherms according to IUPAC classification CeO_2 catalyst shows H_2 hysteresis loop, $Ce_{0.5}Zr_{0.5}O_2$ shows H_1 hysteresis loop and ZrO_2 catalyst shows H_2 hysteresis loop in the relative pressure (P/P_0) range of 0.4−0.95 characteristic for mesoporous materials [39-42].

Basic properties of CeO_2, $Ce_{0.5}Zr_{0.5}O_2$ and ZrO_2 of synthesized catalysts were characterized by CO_2-TPD experiments. Results are shows in Fig 3. Basic properties of catalysts depend upon the temperature profile in weak, moderate and strong range: < 200 °C, 200−450 °C, > 450 °C, respectively. Since all the CeO_2, $Ce_{0.5}Zr_{0.5}O_2$ and ZrO_2 synthesized catalysts show main peaks in the range of 78−117 °C, they contain predominantly week basic sites as shown in Fig 3. Basic sites density (per unit mass of catalysts) of synthesized catalysts was in the order: ZrO_2 (0.2512 mmol/g) < CeO_2 (0.4154 mmol/g) < $Ce_{0.5}Zr_{0.5}O_2$ (0.6487 mmol/g) and basic site density per unit area follows the same order (Table 1). Thus mixed metal oxides are found to posses the basic site density as compared to single oxide catalysts [43]. Zheng et al. [27] and Lee et al. [28] reported maximum CO_2 desorption of 0.276 and 0.017 mmol/g, respectively, for $Ce_{0.6}Zr_{0.4}O_2$ catalysts.

Acidic properties of the CeO_2, $Ce_{0.5}Zr_{0.5}O_2$ and ZrO_2 synthesized catalysts were investigated using NH_3-TPD. Results are shown in Fig. 4b. NH_3 desorption peaks are in temperature region of 50-550 °C. All the catalysts found to contain only week acidic sites. Total desorbed amount of NH_3 was found to be in the following order: $Ce_{0.5}Zr_{0.5}O_2$ > CeO_2 > ZrO_2. The acidic sites density (per unit mass) of synthesized catalysts was in the order: ZrO_2 (0.511 mmol/g) < CeO_2 (0.793 mmol/g) < $Ce_{0.5}Zr_{0.5}O_2$ (1.893 mmol/g). Respective value of acid site density (per unit area) were ZrO_2 (7.3 mmol/m^2) < CeO_2 (9.012 mmol/m^2) < $Ce_{0.5}Zr_{0.5}O_2$ (16.18 mmol/m^2). Therefore, $Ce_{0.5}Zr_{0.5}O_2$ was found to have highest acidic site and ZrO_2 found to have lowest acidic sites in the catalyst. Lee et al. [28] reported much lower NH_3 desorption of 0.0857 mmol/g for $Ce_{0.6}Zr_{0.4}O_2$ catalyst. It may be seen that the $Ce_{0.5}Zr_{0.5}O_2$ catalyst has highest surface area, acidic and basic site density (per unit mass/per unit area) as compared to other CeO_2 and ZrO_2 catalysts. Prepared $Ce_{0.5}Zr_{0.5}O_2$ catalysts posses both basic and acidic sites revealing that it can act as base-acid bi-functional catalyst.

Few researchers have previously reported that both acidic and basic sites are required for direct conversion of CO_2 with methanol to produced DMC [26-28].

3.2 Catalytic activity of catalysts for DMC formation using CO_2

Direct conversion of CO_2 with methanol to form DMC was investigated at different reaction conditions over CeO_2, ZrO_2 and $Ce_{0.5}Zr_{0.5}O_2$ catalysts. It should be mentioned that in the absence of a catalyst, a negligible methanol conversion and DMC formation after 24 h was observed. Results are presented in Fig. 5a. Three catalysts showed different activity in the order ZO_2 < CeO_2 < $Ce_{0.5}Zr_{0.5}O_2$. Among all the catalysts $Ce_{0.5}Zr_{0.5}O_2$ catalyst (2.670 mmol DMC/g.cat.) exhibited the best catalytic activity compared to ZrO_2 (0.456 mmol DMC/g. cat.).

In presence of a suitable catalyst ($Ce_{0.5}Zr_{0.5}O_2$ in the presence case), methanol is activated to form CH_3O^- and H^+ due to acidic and basic site of catalysts [44]. Methoxy species (CH_3O^-) reacts with CO_2 in the presence of basic site and to form methoxyl carbonyl ions. Methanol at the acidic site forms CH_3^+ and OH^- ions. Methoxyl carbonyl ion reacts with CH_3^+ to form DMC and OH^- reacts with H^+ to form of water. As such, higher acidic and basic catalysts facilitate the DMC synthesis from the CO_2 [45]. The reaction mechanism for DMC synthesis from direct conversion of CO_2 with methanol in presence of catalyst can be represented by following equation [45]:

$$CH_3OH \longrightarrow CH_3O^- + H^+ \quad \textbf{Basic site of catalysts reaction}$$

$$CH_3OH \longrightarrow CH_3^+ + OH^- \quad \textbf{Acidic site of catalysts reaction}$$

$$CH_3O^- + CO_2 \longrightarrow CH_3OCO_2^- \quad \textbf{Basic site reaction}$$

$$CH_3OCO_2^- + CH_3^+ \longrightarrow DMC$$

$$H^+ + OH^- \longrightarrow H_2O$$

The relationship between acidic-basic properties and activity of catalysts are shown in Fig. 5b. It can be seen in the above equation, that the acidic and basic properties directly influence the catalytic activity of DMC synthesis. ZrO_2 and CeO_2 have smaller number of acidic and basic sited as compared to $Ce_{0.5}Zr_{0.5}O_2$. It is clearly seen that the DMC yield directly depends upon the acidic-basic properties of catalysts.

The $Ce_{0.5}Zr_{0.5}O_2$ catalyst was further used to study the effects of the reaction conditions such as amount of catalyst, reaction time and reaction temperature for DMC synthesis from CO_2 and methanol.

The effect of reaction time was studied in the range of 6-48 h using $Ce_{0.5}Zr_{0.5}O_2$ catalyst with all other reaction conditions being constant. Results are shown in Fig. 6a. It can be seen that an increase in the reaction time from 6 to 24 h increased the DMC yield from 1.49 to 2.67 mmol/g. After 24 h, DMC yield was constant. It could be observed in Fig 6a that the DMC yield and methanol conversion at 24 h is optimum. It may be due to the saturation of molecular sieve for adsorption of water.

The influence of catalysts dose was studied in the range of 0.62-2.19 g and the results are shown in Fig. 6b. It can be observed in the Fig. 6b, there are distinct trends in methanol conversion and DMC yield with increase in the catalyst amount from 0.6-1.25 g. DMC yield increases from 1.71 to 2.68 mmol/g.cat with increase in the catalyst amount from 0.6-1.25 g. Hereafter, DMC yield decreases with increases in the catalyst amount from 1.86-2.19 g. Maximum DMC yield was found with 1.25 g of catalyst.

The effect of reaction temperature was studied in the temperature (Fig. 6c) range of 120-180 °C. It can be seen that an increase in reaction temperature from 100 to 120 °C increased the DMC yield from 1.249 to 2.682 mmol/g. After that DMC yield decreases to 0.129 mmol/g at 180 °C. Clearly, it can be seen that the optimum in DMC yield was at 120 °C. Further increase in reaction temperature decreases the DMC yield due to the poor

solubility of CO_2 in methanol at higher temperature and also DMC gets decomposed at higher temperature [46,47].

The reusability of $Ce_{0.5}Zr_{0.5}O_2$ catalyst was studied at optimum reaction condition such as catalyst amount=1.25 g, T=120 °C and reaction time=24 h. For this, the $Ce_{0.5}Zr_{0.5}O_2$ catalyst was used in five consecutive batch reactions (Fig. 7). The observed DMC yield and methanol conversion slightly decreased with an increase in reuse cycles. DMC yield and methanol conversion in third run was found to be: 2.6789 mmol/g and 0.78454 mmol/g, respectively. This slight loss of activity of $Ce_{0.5}Zr_{0.5}O_2$ catalyst may be due to the blockage of the pores and active sites deposition of reaction products.

Table 3 compares various catalysts used for synthesis of DMC by direct conversion of CO_2 at various reaction conditions in terms of CO_2 conversion (%) and DMC yield (mmol). It may be seen that the $Ce_{0.5}Zr_{0.5}O_2$ catalyst used in the present study show better or comparable yield and CO_2 conversion with those reported in the literature.

3.3 *Chemical equilibrium modeling*

For the direct synthesis of DMC, equilibrium conversion can be related to the equilibrium constant as shown below:

$$K_{eq}(T) = \frac{a_{DMC}a_{H_2O}}{a_{MeOH}^2 a_{CO_2}}$$

$$= \frac{\frac{1}{2}X_{eq,MeOH}^2\left(1\text{-}0.5y_{MeOH,0}X_{eq,MeOH}\right)}{y_{MeOH,o}\left(1\text{-}X_{eq}\right)^2\left(\Theta_{CO_2}\text{-}\frac{1}{2}X_{eq}\right)} \times \left(\frac{\varphi_{DMC}\varphi_{H_2O}}{(\varphi_{MeOH})^2\varphi_{CO_2}}\right)_{eq}\left(\frac{(\varphi^0_{MeOH})^2\varphi^0_{CO_2}}{\varphi^0_{DMC}\varphi^0_{H_2O}}\right)\left(\frac{P^0}{P}\right) \quad (2)$$

where, $\Theta_{CO_2} = y_{CO_2,0}/y_{MeOH,o}$. The Peng–Robinson–Stryjek–Vera equation of state (PRSV-EoS) [48] along with the van der Waals one-fluid (1PVDW) mixing rule [49], were used to calculate the rules fugacity coefficient of species in the mixture. PRSV-EoS is given as:

$$P = \frac{RT}{V-b} - \frac{a\alpha(T)}{V(V+b)+b(V-b)} \quad (3)$$

where, T_c and P_c are the critical temperature and pressure, respectively, ω is the accentric factor and K is a specific pure compound parameter. The values of T_c, P_c, ω and K as obtained from the literature [49,50] are compiled in Table S2. Values of parameters for 1PVDW model are given in Table S3. More details of PRSV-EoS and 1PVDW are given in supporting information.

PRSV-EoS and 1PVDW model equations along with their parameters and the experimental data obtained in the present study were solved simultaneously to calculate the values of K_{eq} at different temperatures and a constant pressure (P=150 bar) for $Ce_{0.5}Zr_{0.5}O_2$ catalyst. The values K_{eq} are given in Table 2.

Assuming that the heat of reaction ΔH_r^o is constant within the temperature range of 100-180 °C, the equilibrium constant K_{eq} can be related to the T by the classical van't Hoff equation:

$$\ln K_{eq,T} = -\frac{\Delta H_r^o}{RT} + \left(\frac{\Delta H_r^o - \Delta G_r^o}{RT^o} \right) \quad (4)$$

The values of ΔH_r^o and ΔG_r^o for $Ce_{0.5}Zr_{0.5}O_2$ using the data points at T=120-160 °C were found to be −45.66 kJ/mol and 25.04 kJ/mol, respectively. Kongpanna et al. [51] shows the values of ΔH_r^o and ΔG_r^o at 25 °C were found to be −15.259 kJ/mol and 29.583 kJ/mol, respectively.

4. Conclusion

In the present study, DMC was produced by direct conversion of CO_2 with methanol using three different catalysts namely CeO_2, ZrO_2 and $Ce_{0.5}Zr_{0.5}O_2$ catalysts in presence of activated molecular sieve 3A as dehydrating agent. CeO_2, ZrO_2 and $Ce_{0.5}Zr_{0.5}O_2$ catalysts were synthesized by hydrothermal method and characterized using various techniques. CeO_2 catalysts showed reflections of cubic phase with average crystalline sizes 7.09 nm, ZrO_2

catalysts showed reflections of tetragonal phase with average crystalline sizes 9.45 nm and $Ce_{0.5}Zr_{0.5}O_2$ showed tetragonal phase with average crystalline sizes 7.09 nm. BET surface area of CeO_2, ZrO_2 and $Ce_{0.5}Zr_{0.5}O_2$ were found to be 88, 70, and 117 $m^2\ g^{-1}$, respectively. $Ce_{0.5}Zr_{0.5}O_2$ catalyst showed the highest surface area, specific pore volume and average pore diameter among all the synthesized catalysts. The basic sites density and acidic site density of synthesized catalysts was in the order: $ZrO_2 < CeO_2 < Ce_{0.5}Zr_{0.5}O_2$; and that the basic and acidic site density per unit area followed the similar order. DMC production was found to be highly dependent on the acid and base sites of the catalysts. Under optimized reaction condition of reaction temperature=120 °C, reaction time=24 h, catalysts dose=1.25 g with pressure=150 bar, optimum yield of DMC was obtained as 2.56 mmol/g-cat for $Ce_{0.5}Zr_{0.5}O_2$. The values of the heat of reaction (ΔH_r^o) and Gibbs free energy change (ΔG_r^o) for $Ce_{0.5}Zr_{0.5}O_2$ were found to be -45.66 kJ/mol and 25.04 kJ/mol, respectively.

Acknowledgments

One of the authors, namely Praveen Kumar, is thankful to Deutscher Akademischer Austausch Dienst (DAAD), Germany, for providing financial support to carry out this work under a Sandwich Model Scholarship.

References

[1] N. Keller, G. Rebmann, V. Keller, Catalysts, mechanisms and industrial processes for the dimethylcarbonate synthesis, J. mol. Catal. A: Chem. 317 (2010) 1–18.

[2] D. Delledonne, F. Rivetti, U. Romano, Developments in the production and application of dimethylcarbonate, Appl. Catal. A: Gen. 221 (2001) 241–251.

[3] P. Kumar, V. C. Srivastava, I. M. Mishra, Synthesis and characterization of Ce–La oxides for formation of dimethyl carbonate by transesterification of propylene carbonate, Catal. Commun. 60 (2015) 27–31.

[4] Z. Li, B. Cheng, K. Su, Y. Gu, P. Xi, M Guo, The synthesis of diphenyl carbonate from dimethyl carbonate and phenol over mesoporous MoO_3/SiMCM-41, J. Mol. Catal. A: Chem. 289 (2008) 100–105.

[5] L. Torrente-Murciano, A. Gilbank, B. Puertolas, T. Garcia, B. Solsona, D. Chadwick, Shape-dependency activity of nanostructured CeO_2 in the total oxidation of polycyclic aromatic hydrocarbons, Appl. Catal. B: Environ. 132–133 (2013) 116–122.

[6] A. Bansode, A. Urakawa, Towards full one-pass conversion of carbon dioxide to methanol and methanol-derived products, J. Catal. 309 (2014) 66-70.

[7] Y. Zhang, D. N. Briggs, E. De Smit, A.T. Bell, Effects of zeolite structure and composition on the synthesis of dimethyl carbonate by oxidative carbonylation of methanol on Cu-exchanged Y, ZSM-5, and Mordenite, J. Catal. 251 (2007) 443-452.

[8] P. Kumar, V. C. Srivastava, I. M. Mishra, Dimethyl carbonate synthesis by transesterification of propylene carbonate with methanol: Comparative assessment of Ce-M (M=Co, Fe, Cu and Zn) catalysts. Renewable Energy 88 (2016) 457–464.

[9] Z. Hou, L. Luo, K. Liu, C. Liu, Y. Wang, L. Dai, High-yield synthesis of dimethyl carbonate from the direct alcoholysis of urea in supercritical methanol, Chem. Eng. J. 236 (2014) 415–418.

[10] P. Kumar, V. C. Srivastava, I. M. Mishra, Dimethyl carbonate synthesis from propylene carbonate with methanol using Cu-Zn-Al catalyst. Energy Fuels 29(4) (2015) 2664–2675.

[11] J. Bian, X.W. Wei, Y.R. Jin, L. Wang, D.C. Luan, Z.P. Guan, Direct synthesis of dimethyl carbonate over activated carbon supported Cu-based catalysts, Chem. Eng. J. 165 (2010) 686–692

[12] P. Kumar, P. With, V. C. Srivastava, R. Gläser, I. M. Mishra. Conversion of carbon dioxide along with methanol to dimethyl carbonate over ceria catalyst. J. Environ. Chem. Eng. 3 (2015) 2943–2947.

[13] H. Wang, M. Wang, S. Liu, N. Zhao, W. Wei, Y. Sun, Influence of preparation methods on the structure and performance of $CaO–ZrO_2$ catalyst for the synthesis of dimethyl carbonate via transesterification, J. Mol. Catal. A: Chem. 258 (2006) 308–312.

[14] B. Zou, L. Hao, L. Y. Fan, Z. M. Gao, S. L. Chen, H. Li, C. W. Hu, Highly efficient conversion of CO_2 at atmospheric pressure to cyclic carbonates with in situ-generated homogeneous catalysts from a copper-containing coordination polymer, J. Catal. 329 (2015) 119-129.

[15] C. Genovese, C. Ampelli, S. Perathoner, G. Centi, Electrocatalytic conversion of CO_2 on carbon nanotube-based electrodes for producing solar fuels, J. Catal. 308 (2013) 237-249.

[16] Y. Zhang, A. T. Bell, The mechanism of dimethyl carbonate synthesis on Cu-exchanged zeolite Y, J. Catal. 255 (2008) 153–161.

[17] Z.M. Cui, Z. Chen, C.Y. Cao, W.G. Song, L. Jiang, Coating with mesoporous silica remarkably enhances the stability of the highly active yet fragile flower-like MgO catalyst for dimethyl carbonate synthesis, Chem. Commun. 49 (2013) 6093-6095.

[18] J. Holtbruegge, M. Wierschem, P. Lutze, Synthesis of dimethyl carbonate and propylene glycol in a membrane-assisted reactive distillation process: Pilot-scale

experiments, modeling and process analysis, Chem. Eng. Process.: Process Intensif. 84 (2014) 54-70.

[19] P. Svec, R. Olejník, Z. Padelková, A. Ruzicka, L. Plasseraud, C,N-chelated organotin(IV) trifluoromethanesulfonates: Synthesis, characterization and preliminary studies of its catalytic activity in the direct synthesis of dimethyl carbonate from methanol and CO_2, J. Organometallic Chem. 708-709 (2012) 82-87.

[20] J.F. Knifton, R.G. Duranleau, Ethylene glycol—dimethyl carbonate cogeneration, J. Mol. Catal. 67 (1991) 389–399.

[21] S. Fang, K. Fujimoto, Direct synthesis of dimethyl carbonate from carbon dioxide and methanol catalyzed by base, Appl. Catal. A: Gen. 142 (1996) L1-L3.

[22] J. Kizlink, Synthesis of dimethyl carbonate from carbon dioxide and methanol in the presence of organotin compounds, Collect. Czech. Chem. Commun. 58 (1993) 399-1402.

[23] J. Kizlink, I. Pastucha, Preparation of Dimethyl carbonate from methanol and carbon dioxide in the presence of Sn(IV) and Ti(IV) alkoxides and metal acetates, Collect. Czech. Chem. Commun. 60 (1995) 687-692.

[24] B. Zhao, Y. X. Pan, C. J. Liu, The promotion effect of CeO_2 on CO_2 adsorption and hydrogenation over Ga_2O_3, Catal. Today 194 (2012) 60-64.

[25] W. Wang, Y. Zhang, Z. Wang, J. M. Yan, Q. Ge, C. J. Liu, Reverse water gas shift over In_2O_3-CeO_2 catalysts, Catal. Today http://dx.doi.org/10.1016/j.cattod.2015.0403 2.

[26] L. Chen, S. Wang, J. Zhou, Y. Shen, Y. Zhao, X. Ma, Dimethyl carbonate synthesis from carbon dioxide and methanol over CeO_2 versus over ZrO_2: comparison of mechanisms. RSC Adv.4 (2014) 30968-30975.

[27] Z.F. Zhang, Z.T. Liu, Z.W. Liu, J. Lu, DMC formation over $Ce_{0.5}Zr_{0.5}O_2$ prepared by complex-decomposition method, Catal. Lett. 129 (2009) 428–436.

[28] H.J. Lee, W. Joe, I.K. Song, Direct synthesis of dimethyl carbonate from methanol and carbon dioxide over transition metal oxide/$Ce_{0.6}Zr_{0.4}O_2$ catalysts: Effect of acidity and basicity of the catalysts. Korean J. Chem. Eng. 29 (2012) 317-322.

[29] S. Wada, K. Oka, K. Watanable, Y. Izumi, Catalytic conversion of carbon dioxide into dimethyl carbonate using reduced copper-cerium oxide catalysts as low as 353 K and 1.3 MPa and the reaction mechanism, Frontiers in Chem. 1 (2013) 1-8.

[30] D. Ballivet-Tkatchenko, F. Bernard, F. Demoisson, L. Plasseraud, S.R. Sanapureddy, Tin-based mesoporous silica for the conversion of CO_2 into dimethyl carbonate, ChemSusChem 4 (2011) 1316–1322.

[31] R. O. Fuentes, R.T. Baker, Synthesis of nanocrystalline CeO_2-ZrO_2 solid solutions by a citrate complexation route: A thermochemical and structural study, J. Phys. Chem. C 113 (2009) 914–924.

[32] S. Brunauer, P. H. Emmet, F. Teller, Adsorption of gases in multimolecular layers, J. Am. Chem. Soc. 60 (1938) 309- 319.

[33] E. P. Barret, L. G. Joyner, P. P. Hanlenda, The Determination of Pore Volume and Area Distributions in Porous Substances. I. Computations from Nitrogen Isotherms, J. Am. Chem. Soc.73 (1951) 373-380.

[34] R Si, Y. W. Zhang, L. M. Wang, S. J. Li, B. X. Lin, W. S. Chu, Z. Y. Wu, C. H. Yan, Enhanced thermal stability and oxygen storage capacity for $Ce_xZr_{1-x}O_2$ (x=0.4-0.6) solid solutions by hydrothermally homogenous doping of trivalent rare earths. J. Phys. Chem. C 111 (2007) 787-794.

[35] H. S. Roh, I. H. Eum, D. W. Jeong, Low temperature steam reforming of methane over Ni– $Ce_{(1-x)}Zr_{(x)}O_2$ catalysts under severe conditions, Renew. Energy. 42 (2012) 212-216.

[36] I. Atribak, A. Bueno-Lopez, A. Garcia-Garcia, Combined removal of diesel soot particulates and NOx over CeO_2–ZrO_2 mixed oxides, J. Catal. 259 (2008) 123-132.

[37] I. Atribak, I. Such-Basáñez, A. Bueno-López, A. García, Comparison of the catalytic activity of MO_2 (M = Ti, Zr, Ce) for soot oxidation under NOx/O_2, J. Catal. 250 (2007) 75-84.

[38] J. M. López, A. L. Gilbank, T. García, B. Solsona, S. Agouram, L. Torrente-Murciano, The prevalence of surface oxygen vacancies over the mobility of bulk oxygen in nanostructured ceria for the total toluene oxidation, Appl. Catal. B: Environ. 174–175 (2015) 403–412.

[39] J. Ouyang, J. Jin, H. Yang, A. Tang, A complex and de-complex strategy to ordered mesop orous $Ce_{0.5}Zr_{0..5}O_2$ with comprehensive pilot scale performances, Mat. Chem. Phy. 147 (2014) 1009-1015.

[40] A. Pineda, A. M. Balu, J. M. Campelo, A. A. Romero, D. Carmona, F. Balas, J. Santamaria, R. Luque, A dry milling approach for the synthesis of highly active nanoparticles supported on porous materials, ChemSusChem 4 (2011) 1561–1565.

[41] B. Samojeden, M. Motak, T. Grzybek, The influence of the modification of carbonaceous materials on their catalytic properties in SCR-NH_3. A short review, C. R. Chimie (2015), http://dx.doi.org/10.1016/j.crci.2015.04.001

[42] N. Guillén-Hurtado, A. García-García, A. Bueno-López, Isotopic study of ceria-catalyzed soot oxidation in the presence of NOx, J. Catal. 299 (2013) 181-187.

[43] K.W. La, J.C. Jung, H. Kim, S.H. Baeck, I.K. Song, Effect of acid–base properties of $H_3PW_{12}O_{40}/Ce_xTi_{1-x}O_2$ catalysts on the direct synthesis of dimethyl carbonate from

methanol and carbon dioxide: A TPD study of $H_3PW_{12}O_{40}/Ce_xTi_{1-x}O_2$ catalysts, J. Mol. Catal. A: Chem. 269 (2007) 41–45.

[44] Y. Zhou, S. Wang, M. Xiao, D. Han, Y. Lu, Y. Meng, Novel Cu–Fe bimetal catalyst for the formation of dimethyl carbonate from carbon dioxide and methanol, RSC Adv. 2 (2012) 6831–6837.

[45] K. Almusaiteer, Synthesis of dimethyl carbonate (DMC) from methanol and CO_2 over Rh-supported catalysts, Catal. Commun. 10 (2009) 1127-1131.

[46] S. Kumar, S.L. Jain, Polyethylene glycol enfolded KBr assisted base catalyzed synthesis of dimethyl carbonate from methanol and carbon dioxide, Ind. Eng. Chem. Res. 53 (2014) 15798−15801.

[47] B. Zhao, Y. X. Pan, C. J. Liu, The promotion effect of CeO_2 on CO_2 adsorption and hydrogenation over Ga_2O_3, Catal. Today 194 (2012) 60-64.

[48] R. Stryjek, J. H. Vera, PRSV: An improved Peng—Robinson equation of state for pure compounds and mixtures, Can. J. Chem. Eng. 64 (1986) 323–333.

[49] R. Piñero, J. García, M. Sokolova, M. J. Cocero, Modelling of the phase behaviour for the direct synthesis of dimethyl carbonate from CO_2 and methanol at supercritical or near critical conditions, The Journal of Chemical Thermodynamics 39 (2007) 536–549

[50] F. Bustamente, A. F. Orrego, S. Villegas, A. L. Villa, Modeling of chemical equilibrium and gas phase behavior for the direct synthesis of dimethyl carbonate from CO_2 and methanol. Ind. Eng. Chem. Res. 51 (2012) 8945−8956.

[51] P. Kongpanna, V. Pavarajarn, R. Gani, S. Assabumrungrat, Techno-economic evaluation of different CO_2-based processes for dimethyl carbonate production. Chem. Eng res. Des. 93 (2015) 496–510.

Table 1. Crystallite size, textural CO_2-TPD and NH_3-TPD analysis of CeO_2, $Ce_{0.5}Zr_{0.5}O_2$ and ZrO_2 catalysts.

Catalysts Properties	CeO_2	$Ce_{0.5}Zr_{0.5}O_2$	ZrO_2
Crystallite size (nm)[a]	9.48	7.09	9.45
Lattice constant d (nm)[a]	0.3124	0.3051	0.2950
BET surface area (m^2/g)	88	117	70
Specific pore volume ($cm^3\ g^{-1}$)[b]	0.12	0.237	0.202
Average Pore diameter (nm)[c]	5	8.41	7.89
CO_2 adsorption ($mmol.g^{-1}$)[d]	0.4154 (117)	0.6487 (88)	0.2512 (78)
Basic site density ($\mu mol.m^{-2}$) [d]	4.721	5.550	3.588
NH_3 adsorption ($mmol.g^{-1}$)[e]	0.793 (110)	1.893 (96)	0.511 (93)
Acidic site density ($\mu mol.m^{-2}$)[e]	9.012	16.18	7.3

[a]Crystallite size and lattice constant are calculated by Scherrer equation.

[b]BJH desorption cumulative pore volume of pores in the range 17 to 3000 Å.

[c]BJH desorption average pore diameter.

[d]CO_2-TPD of for basicity and basic site and temperature (°C) at maxima is given in brackets.

[e]NH_3-TPD of for acidity and acidic site and temperature (°C) at maxima is given in brackets.

Table 2. Values of K_{eq} for DMC synthesis by direct CO_2 conversion using $Ce_{0.5}Zr_{0.5}O_2$ catalyst at different temperatures and a constant pressure, P=150 bar.

T (K)	$y_{o,MeOH}$	$y_{o,\ CO2}$	$X_{eq,MeOH,\ experimental}$	$y_{eq,MeOH}$	$y_{eq,\ CO2}$	$y_{eq,DMC}$	$y_{eq,H2O}$	K_{eq} (l/mol)
353	0.686055	0.313945	0.00330459	0.684985	0.313975	0.000519638	0.000519638	3.930×10^{-8}
373	0.697797	0.302203	0.0072792	0.695485	0.302307	0.001104294	0.001104294	2.221×10^{-7}
393	0.708692	0.291308	0.00945482	0.705748	0.291483	0.001384505	0.001384505	4.313×10^{-7}
413	0.718828	0.281172	0.00687782	0.716735	0.281324	0.000970785	0.000970785	2.608×10^{-7}
433	0.728283	0.271717	0.0050323	0.726785	0.271843	0.000685724	0.000685724	1.620×10^{-7}
453	0.737123	0.262877	0.00288836	0.736282	0.262957	0.000380307	0.000380307	6.370×10^{-8}

Table 3. Comparison of various catalysts used for synthesis of DMC by direct conversion of CO_2 at various reaction conditions.

Catalyst @ Preparation Method	Reaction Condition	CO_2 moles (mmol)	%Conversion of CO_2	DMC Yield (mmol)	Reference
Sonicated Sn-SBA-15@ Template	P=20 MPa, T=423 K, t=15h, m=0.1	604	0.268	0.81	[30]
Sn-SBA-15@ Template	P=20 MPa, T=423 K, t=15h, m=0.1	604	0.099[@]	0.3	[30]
$Ce_{0.4}Zr_{0.6}O_2$@ Sol-gel	P=6 MPa, T =443 K, t=3h, m=0.7 g	123	0.324[@]	0.7	[28]
Gd-$Ce_{0.4}Zr_{0.6}O_2$@ Sol-gel	P=6 MPa, T=443 K, t=3h, m=0.7 g	123	1.131[@]	0.7	[28]
Cu-CeO_2@ Impregnation	P=62.8MPa, T=393, t=4h, m=0.1 g	134	0.598[@]	0.4	[29]
CeO_2@ Sol-gel	P=5 MPa, T=413 K, t=2h, m=0.1 g	145.57	0.724[@]	0.534	[26]
ZrO_2@ Sol-gel	P=5 MPa, T=413 K, t=2h, m=0.1 g	145.57	0.028[@]	0.021	[26]
CeO_2@ Hydrothermal	P=15 MPa, T=393K, t=24 h, m=1.25 g	294	1.39	2.04	This work
ZrO_2@ Hydrothermal	P=15 MPa, T=393K, t=24 h, m=1.25 g	294	0.51	0.45	This work
$Ce_{0.5}Zr_{0.5}O_2$@ Hydrothermal	P=15 MPa, T=393K, t=24 h, m=1.25 g	294	1.82	2.67	This work

[@]Calculated from conditions given in the respective literature. P: Pressure; T: temperature; t: time; m: mass of catalyst.

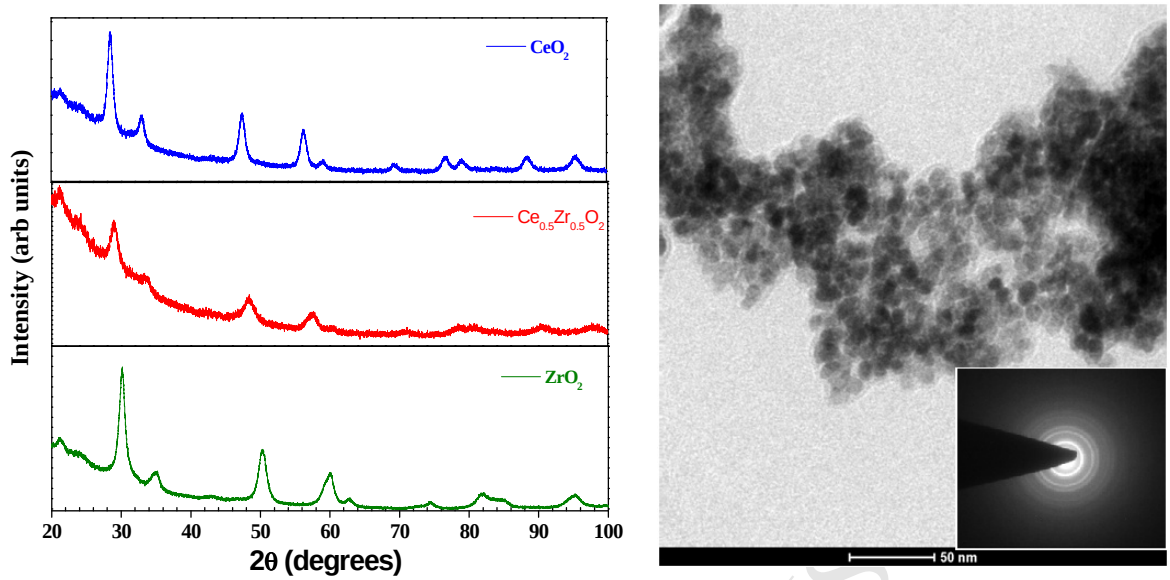

(a) (b)

Fig. 1. (a) XRD pattern of CeO_2, $Ce_{0.5}Zr_{0.5}O_2$ and ZrO_2 catalysts and; (b) TEM image of $Ce_{0.5}Zr_{0.5}O_2$ catalyst with SEAD patterns.

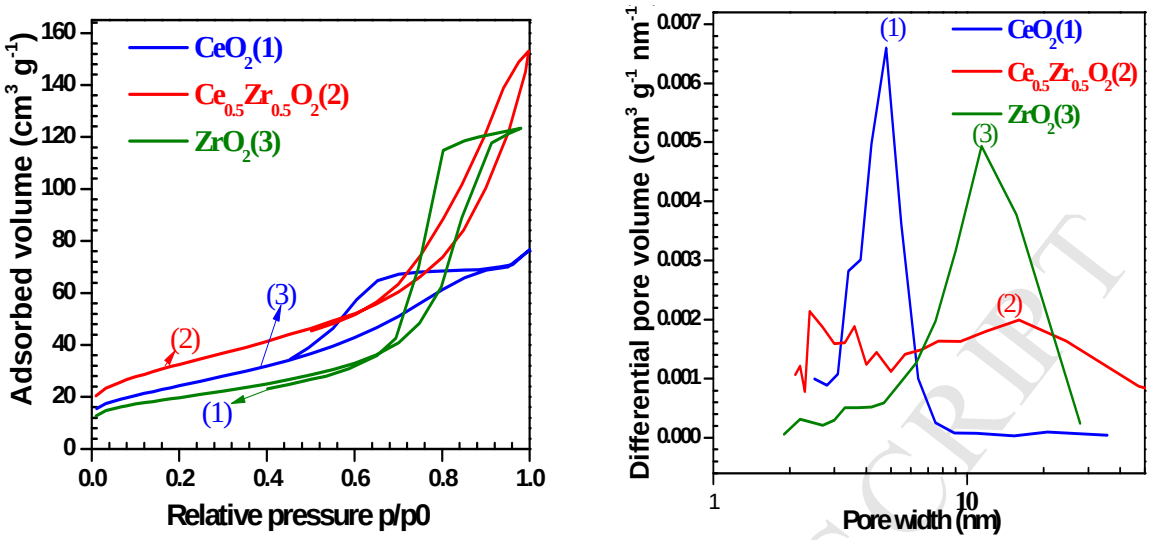

(a) (b)

Fig. 2. (a) Nitrogen adsorption-desorption isotherms; (b). Variation of pore volume and pore area with pore diameter of CeO_2, $Ce_{0.5}Zr_{0.5}O_2$ and ZrO_2 catalysts.

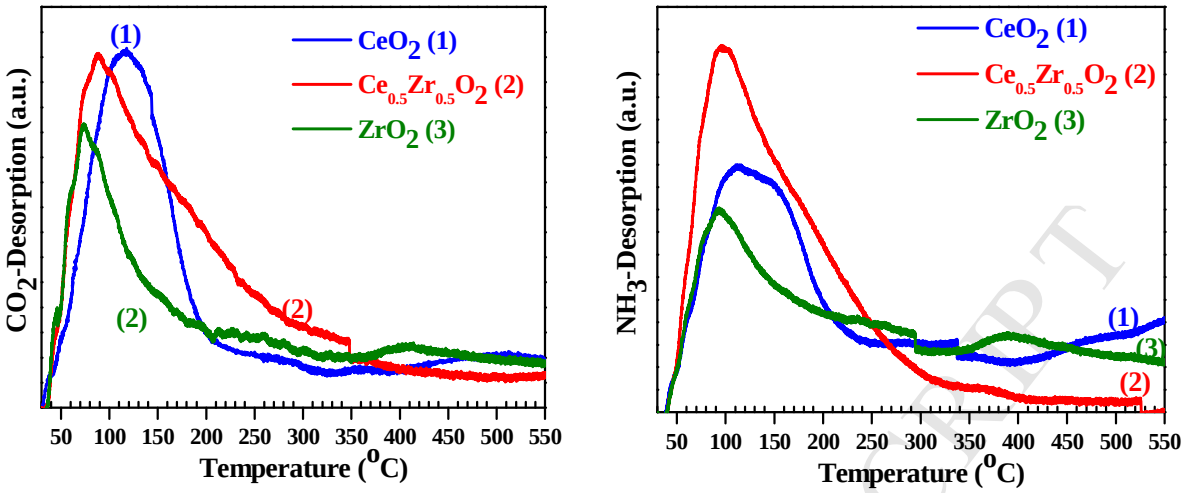

(a) (b)

Fig. 3. (a). CO_2-TPD; (b). NH_3-TPD of CeO_2, $Ce_{0.5}Zr_{0.5}O_2$ and ZrO_2 catalysts.

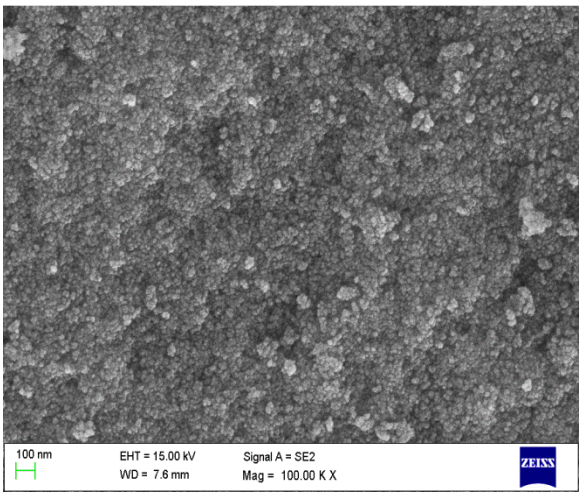

CeO_2

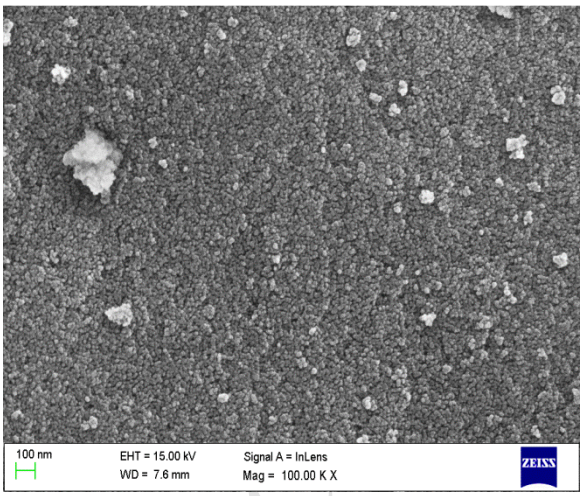

ZrO_2

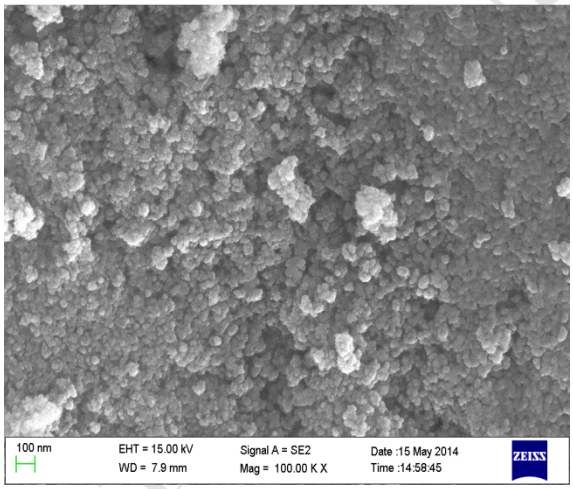

$Ce_{0.5}Zr_{0.5}O_2$

Fig. 4 SEM image of CeO_2, ZrO_2 and $Ce_{0.5}Zr_{0.5}O_2$ catalysts.

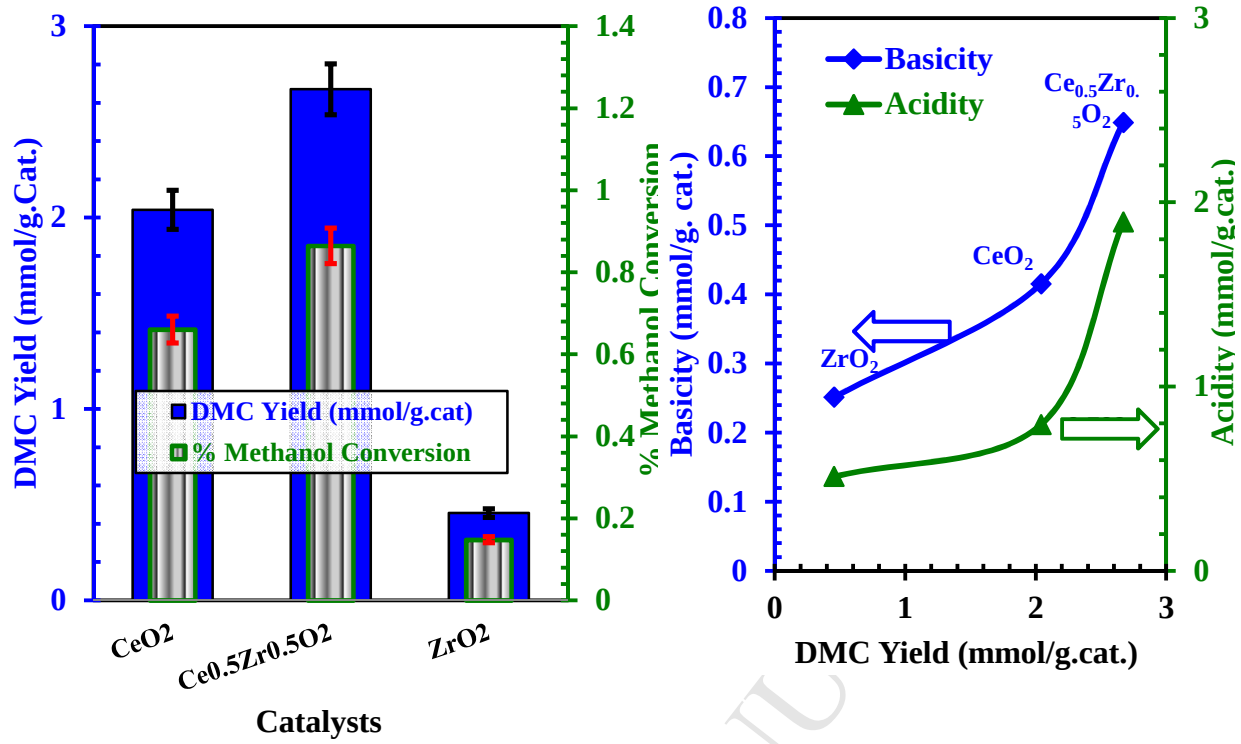

(a) **(b)**

Fig. 5. (a) Methanol Conversion and DMC yield over CeO_2, $Ce_{0.5}Zr_{0.5}O_2$ and ZrO_2 catalysts; (b) Correlation between acidic-basic and catalytic activity of CeO_2, $Ce_{0.5}Zr_{0.5}O_2$ and ZrO_2 catalysts; Reaction conditions: (Methanol=25.03 ml, $m_{catalyst\ dose}$=1.25 g, P=150 bar, T=120 °C, t_r=24 h).

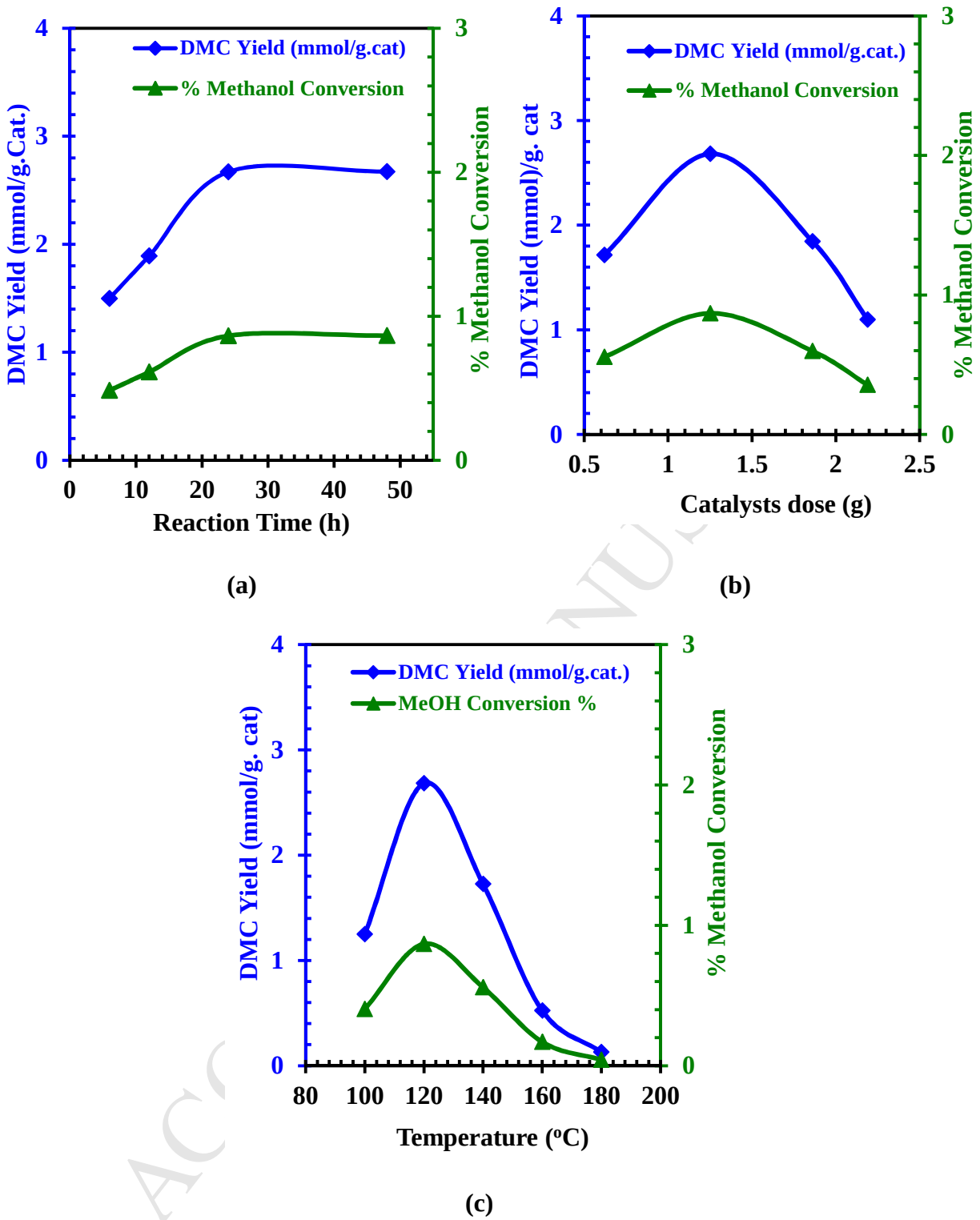

Fig. 6. Effect of various parameters for direct conversion of CO_2 with methanol for DMC synthesis. (a) effect of reaction time at Methanol=25.03 ml, $m_{catalyst\ dose=}$1.25 g, P=150 bar, T=120 °C; (b) effect of catalyst dose at Methanol=25.03 ml, P=150 bar, T=120 °C, t_r=24 h; and (c) effect of temperature at Methanol=25.03 ml, $m_{catalyst\ dose=}$1.25 g, P=150 bar.

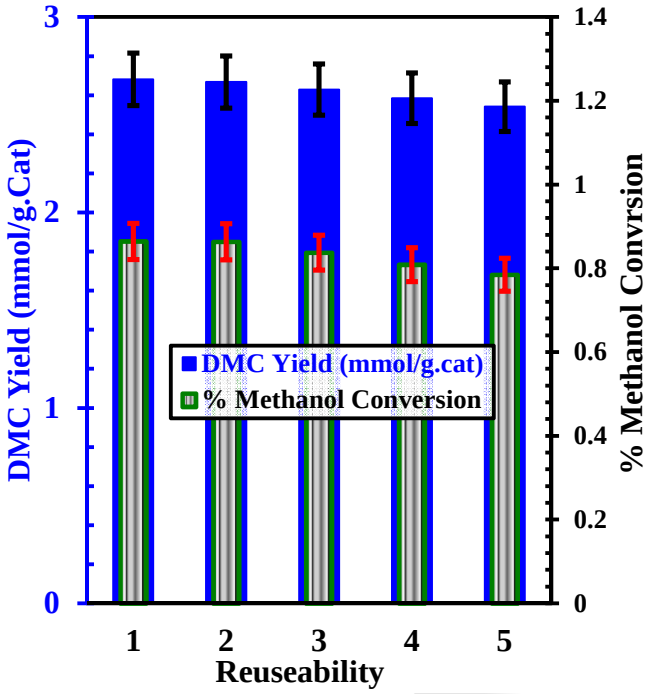

Fig. 7. Reuseability of $Ce_{0.5}Zr_{0.5}O_2$ catalyst DMC synthesis from direct conversion of CO_2 with methanol: (Methanol=25.03 ml, $m_{catalyst\ dose}$=1.25 g, P=150 bar, T=120 °C, t_r=24 h).

Figures Captions

Fig. 1. (a) XRD pattern of CeO_2, $Ce_{0.5}Zr_{0.5}O_2$ and ZrO_2 catalysts and; (b) TEM image of $Ce_{0.5}Zr_{0.5}O_2$ catalyst with SEAD patterns.

Fig. 2. (a) Nitrogen adsorption-desorption isotherms; (b). Variation of pore volume and pore area with pore diameter of CeO_2, $Ce_{0.5}Zr_{0.5}O_2$ and ZrO_2 catalysts.

Fig. 3. (a). CO_2-TPD; (b). NH_3-TPD of CeO_2, $Ce_{0.5}Zr_{0.5}O_2$ and ZrO_2 catalysts.

Fig. 4 SEM image of CeO_2, ZrO_2 and $Ce_{0.5}Zr_{0.5}O_2$ catalysts.

Fig. 5. (a) Methanol Conversion and DMC yield over CeO_2, $Ce_{0.5}Zr_{0.5}O_2$ and ZrO_2 catalysts; (b) Correlation between acidic-basic and catalytic activity of CeO_2, $Ce_{0.5}Zr_{0.5}O_2$ and ZrO_2 catalysts; Reaction conditions: (Methanol=25.03 ml, $m_{catalyst\ dose=}$1.25 g, P=150 bar, T=120 °C, t_r=24 h).

Fig. 6. Effect of various parameters for direct conversion of CO_2 with methanol for DMC synthesis. (a) effect of reaction time at Methanol=25.03 ml, $m_{catalyst\ dose=}$1.25 g, P=150 bar, T=120 °C; (b) effect of catalyst dose at Methanol=25.03 ml, P=150 bar, T=120 °C, t_r=24 h; and (c) effect of temperature at Methanol=25.03 ml, $m_{catalyst\ dose=}$1.25 g, P=150 bar.

Fig. 7. Reuseability of $Ce_{0.5}Zr_{0.5}O_2$ catalyst DMC synthesis from direct conversion of CO_2 with methanol: (Methanol=25.03 ml, $m_{catalyst\ dose=}$1.25 g, P=150 bar, T=120 °C, t_r=24 h).

RESEARCH HIGHLIGHTS

> Cerium-Zirconium catalysts prepared by hydrothermal method. > Catalysts characterized by XRD, CO_2- & NH_3-TPD, N_2 adsorption and SEM techniques. > Direct conversion of CO_2 to produced dimethyl carbonate. > Optimization of catalyst dose, reaction time and reaction temperature. > Thermodynamics study. >